nature neuroscience

Input normalization by global feedforward inhibition expands cortical dynamic range

Frédéric Pouille[1,2], Antonia Marin-Burgin[1,2], Hillel Adesnik[1], Bassam V Atallah[1] & Massimo Scanziani[1]

The cortex is sensitive to weak stimuli, but responds to stronger inputs without saturating. The mechanisms that enable this wide range of operation are not fully understood. We found that the amplitude of excitatory synaptic currents necessary to fire rodent pyramidal cells, the threshold excitatory current, increased with stimulus strength. Consequently, the relative contribution of individual afferents in firing a neuron was inversely proportional to the total number of active afferents. Feedforward inhibition, acting homogeneously across pyramidal cells, ensured that threshold excitatory currents increased with stimulus strength. In contrast, heterogeneities in the distribution of excitatory currents in the neuronal population determined the specific set of pyramidal cells recruited. Together, these mechanisms expand the range of afferent input strengths that neuronal populations can represent.

A characteristic of cortical excitatory neurons is their widely divergent axonal projection. This property enables cortical neurons to contact a large number of postsynaptic cells and allows each postsynaptic cell to receive inputs from many presynaptic neurons. In a circuit constructed with this excitatory divergence alone, the number of active presynaptic neurons (input strength) that is sufficient to recruit all neurons in the postsynaptic population is only slightly larger than the input strength required to recruit any postsynaptic neuron at all. In other words, the input range that can be faithfully represented by the postsynaptic population is restricted. For example, if presynaptic neurons connect to a postsynaptic population with a probability of 15%[1] and each postsynaptic cell requires 40 active inputs to be recruited[2], then 2% of the postsynaptic cells would be recruited by the activity of 200 presynaptic neurons and almost all (>99%) would be recruited by simply doubling the number of active presynaptic neurons (as determined by binomial statistics). Thus, in the absence of control mechanisms, small fluctuations in the fraction of presynaptically active neurons results in all-or-none recruitment of the postsynaptic population[3–6] (this all-or-none behavior is qualitatively similar for a wide range of connectivity values and number of inputs necessary to reach threshold). However, both spontaneous and sensory-evoked cortical activity involves large fluctuations in the fraction of active neurons (for example, refs. 7–9). What mechanisms does the cortex use to expand the range of input strengths over which it faithfully responds? One could imagine at least two distinct mechanisms. Reducing the gain of individual neurons (that is, the change in spiking probability as a function of input strength) would allow each neuron in the population to respond over a wider range of input strengths; this gain modulation could be achieved through $GABA_A$ receptor–mediated conductances[10–13]. Alternatively, staggering the recruitment of individual neurons over a wide range of input strengths would allow the population as a whole, rather than individual neurons, to represent a wider input range. This could be achieved by varying the amplitude of the excitatory postsynaptic currents (EPSCs) necessary to reach threshold for spike generation as a function of input strength.

We found that hippocampal and neocortical feedforward inhibitory circuits staggered the recruitment of individual pyramidal cells over a wide range of input strengths. Feedforward inhibition (FFI) acted homogeneously across the postsynaptic population of pyramidal cells to rapidly adjust their excitability to the strength of incoming presynaptic activity. As a result, the amplitude of the EPSC necessary for a pyramidal cell to reach spike threshold was dynamic and varied with the strength of the input. Heterogeneities in the amplitudes of EPSCs across the postsynaptic population determined the specific subset of pyramidal cells that would spike in response to the presynaptic input. Through this coordinated action of direct excitation and FFI, pyramidal cell populations can remain sensitive to weak inputs, but will not saturate in response to stronger activity.

RESULTS

EPSC necessary to spike pyramidal cell is dynamic

We established the range of stimulus strengths over which the CA1 pyramidal cell population responds, that is, the dynamic range. We recorded from individual pyramidal cells in the loose-patch configuration and stimulated Schaffer collaterals over a range of intensities, from those that failed to trigger any spike to those that triggered spikes on every trial (**Fig. 1a**). The relationship between spiking probability of individual pyramidal cells and input strength (input strength is proportional to the number of activated Schaffer collateral; for details see Online Methods and **Supplementary Fig. 1**) was fitted with a sigmoid to interpolate the threshold input strength, where pyramidal cells spiked in 50% of the trials (**Fig. 1a**). The cumulative distribution of threshold input strengths for all recorded pyramidal cells

[1]Howard Hughes Medical Institute and Neurobiology Section, Division of Biology, University of California San Diego, La Jolla, California, USA. [2]These authors contributed equally to this work. Correspondence should be addressed to M.S. (massimo@ucsd.edu).

Received 5 August; accepted 25 September; published online 1 November 2009; doi:10.1038/nn.2441

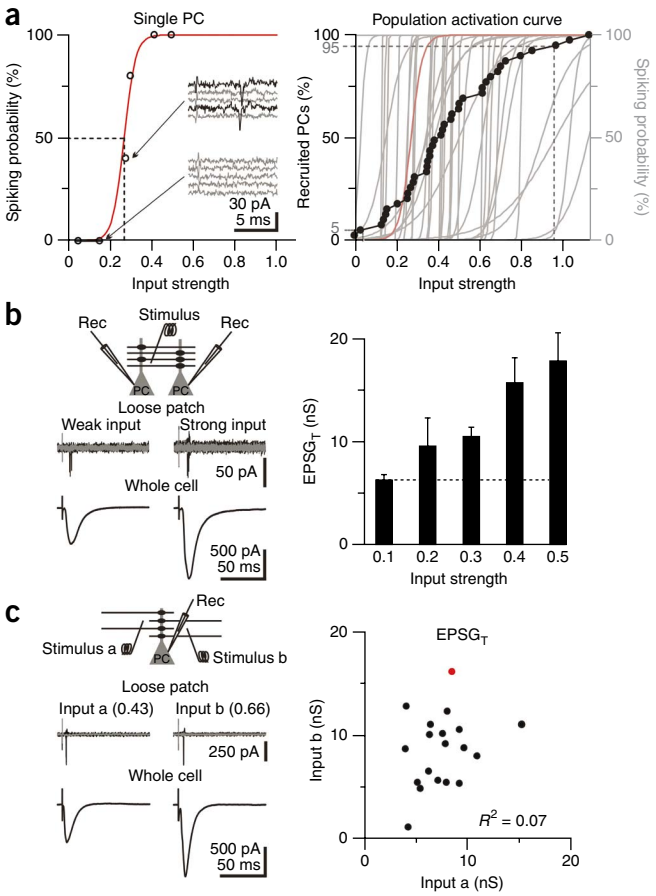

Figure 1 The stronger the stimulus, the larger the excitation necessary to recruit a pyramidal cell. (**a**) Left, spiking probability plotted against input strength for one CA1 pyramidal cell (PC, sigmoidal fit, dashed lines indicate 50% spiking probability). Inset, loose-patch recording at two different input strengths, five consecutive sweeps. Successes are shown in black and failures in gray. Right, black data points represent the activation curve (that is, the cumulative distribution of input strengths eliciting 50% spiking, $n = 39$). Dashed lines represent the input strengths recruiting 5% and 95% of the pyramidal cell population. Gray sigmoids indicate the spiking probability of the 39 pyramidal cells making up the activation curve. Their recruitment was staggered along the range of input strengths. Red sigmoid indicates the experiment shown on the left. (**b**) Top left, recording configuration. Rec, recording electrode. Top traces represent the responses of two CA1 pyramidal cells simultaneously recorded in loose-patch to threshold stimulation of Schaffer collateral inputs (five superimposed sweeps; successes are shown in black, failures in gray). The pyramidal cell on the left was recruited at weaker stimulus than the pyramidal cell on the right. Bottom traces represent threshold EPSCs (that is, EPSCs evoked at threshold input strength, average of ten traces) recorded in the same two cells voltage clamped at –80 mV. The pyramidal cell on the left necessitated less excitation to reach threshold. Right, summary graph of $EPSG_T$s (black, $n = 32$, spike threshold determined in loose patch for $n = 15$ cells and in whole-cell current clamp for $n = 17$ cells) plotted against input strength at threshold (bin width 0.1). Dashed line represents the average $EPSG_T$ for the 0–0.1 bin. Error bars are s.e.m. (**c**) Top left, recording configuration. Top traces represent the response of a single CA1 pyramidal cell recorded in loose patch to threshold stimulation of two different Schaffer collateral inputs (stimuli a and b, five superimposed sweeps each). Bottom traces represent threshold EPSCs (average of ten traces) recorded in the same cell voltage clamped at –90 mV. The difference in amplitude of the two threshold EPSCs should be noted. Right, summary graph ($n = 19$). There was no correlation between $EPSG_T$s evoked by input a and input b (linear regression, $R^2 = 0.07$; spike threshold determined in loose patch for all cells, red data point indicates the experiment shown on the left).

($n = 39$) represents the fractional recruitment of the CA1 pyramidal cell population, or activation curve (**Fig. 1a**). The dynamic range of the pyramidal cell population (that is, the ratio of the input strength necessary to activate 95% versus 5% of the pyramidal cell population) was approximately 34 (**Fig. 1a**), meaning that the pyramidal cell population can differentially represent a 34-fold increase in the number of active Schaffer collateral inputs before saturating. This is much larger than the dynamic range of an individual pyramidal cell (1.6 ± 0.7, $n = 37$; **Fig. 1a**; invariant between pyramidal cells recruited at different input strengths, $R^2 = 0.034$, $P = 0.27$; **Supplementary Fig. 2**) and is the result of staggered recruitment of CA1 pyramidal cells over a wide range of stimulus strengths (**Fig. 1a**).

Why are some pyramidal cells recruited at low input strength, whereas others require much stronger stimuli? We compared the excitatory postsynaptic conductance (EPSG) evoked at threshold input strength[2] of pyramidal cells recruited over the range of input strengths ($EPSG_T$ refers to the EPSG evoked at threshold). **Figure 1b** illustrates an example of two pyramidal cells, simultaneously recorded in the loose-patch configuration, that required different stimulus strengths to spike. Whole-cell, voltage-clamp recording from the same two cells showed that the $EPSG_T$ in the pyramidal cell recruited by the stronger stimulus was much larger than in the pyramidal cell recruited with weaker stimulus (**Fig. 1b**). Over all of the experiments, we observed a steep increase in $EPSG_T$s with increasing input strength (0.3-nS increase per percentile input strength, $n = 32$, $P = 0.0024$; **Fig. 1b**).

The increase in $EPSG_T$ with input strength was not unique to pyramidal cells recruited by single-shock stimulation of the Schaffer collateral. Even when pairs of pyramidal cells were recruited by repetitive high-frequency stimulation (2–6 stimuli at 0.2–0.5 kHz), mimicking bursting activity in CA3, as recorded *in vivo*[14], $EPSG_T$s were significantly larger in the cell recruited with higher input strength (1.7 ± 0.2–fold larger, $n = 12$ pairs, $P = 0.012$; **Supplementary Fig. 3**). This held true for even higher stimulus frequencies (4–6 stimuli at 1 kHz, 1.6 ± 0.2–fold larger, $n = 6$ pairs, $P = 0.045$; **Supplementary Fig. 3**). Thus, pyramidal cells recruited at higher input strengths need larger EPSGs to reach spike threshold.

Are differences in $EPSG_T$ amplitudes the results of variability in intrinsic pyramidal cell properties? Input resistance, membrane time constant, resting potential and threshold potential did not significantly differ between pyramidal cells recruited at different input strengths (**Supplementary Fig. 4**). To further rule out the influence of intrinsic variability between pyramidal cells, we compared $EPSG_T$s between two independent Schaffer collateral inputs converging onto a single pyramidal cell (**Fig. 1c**). $EPSG_T$s were uncorrelated between the two inputs (**Fig. 1c**). Furthermore, in an individual pyramidal cell, the $EPSG_T$ evoked by the stronger input was invariably larger than the $EPSG_T$ evoked by the weaker input (1.5 ± 0.2–fold larger; $P = 0.002$, $n = 19$; **Fig. 1c**). Finally, there was no significant difference in the rise and decay kinetics of $EPSG_T$s evoked by the weak and strong inputs (10–90% rise time: strong stimulus, 2.8 ± 0.2 ms; weak stimulus, 2.6 ± 0.3 ms; $P = 0.67$, $n = 19$; decay time constant: strong stimulus, 7.0 ± 0.4 ms; weak stimulus, 6.8 ± 0.4 ms; $P = 0.74$, $n = 19$), ruling out differences resulting from the distribution of the excitatory inputs along the somatodendritic axis. Thus, even in an individual pyramidal cell, the $EPSG_T$ varied depending on the activated input, indicating that the same pyramidal cell can be recruited at both the low or high end of the stimulus range.

The increase in $EPSG_T$ implies that the contribution of each individual afferent in firing the neuron decreases with increasing input strength. By how much does this decrease? Over the range of

input strengths from 0 to 0.5, the amplitude of the $EPSG_T$ increased approximately linearly (**Fig. 1b**; see model below) such that

$$EPSG_{TN} = Nk + EPSG_{T0}$$

where N is the number of active afferents, $EPSG_{TN}$ is the $EPSG_T$ when N afferents are active, $EPSG_{T0}$ is the EPSG necessary to reach threshold at minimal input strength (under our condition, it was ~6 nS; **Fig. 1b**) and k is the proportionality factor. Given g, the synaptic conductance produced by an individual afferent, the relative contribution of each afferent toward firing a cell, $\left(\frac{g}{EPSG_{TN}}\right)$, is $\frac{g}{(Nk + EPSG_{T0})}$. Thus, the relative contribution of individual afferents in firing a cell is normalized by the number of active afferents.

FFI expands population's dynamic range

What determines the amplitude of the $EPSG_T$ and why does it vary with input strength? Stimulation of Schaffer collaterals triggers powerful FFI in CA1 pyramidal cells through the recruitment of GABAergic interneurons[15–17]. There was a strong correlation between the amplitude of the $EPSG_T$ and the amplitude of the concomitantly triggered feedforward inhibitory postsynaptic conductance (IPSG; **Fig. 2a**; see Online Methods and **Supplementary Fig. 5**). Furthermore, consistent with the correlation between $EPSG_T$ and input strength (**Fig. 1b**), FFI increased with input strength, before saturating at input values above ~0.5 (**Fig. 2a**). These data suggest that $EPSG_T$ may vary with input strength because of a parallel increase of FFI. We directly tested this possibility by either abolishing GABAergic transmission or by imposing a fixed amount of inhibition (**Fig. 2b**). Abolishing FFI with the $GABA_A$ receptor antagonist gabazine eliminated the increase in $EPSG_T$ with input strength (nonsignificant increase of 0.07 nS per percentile input strength, $n = 30$, $P = 0.22$; **Fig. 2b**), demonstrating a crucial role of $GABA_A$ receptors.

To impose a fixed amount of inhibition, irrespective of input strength (**Fig. 2b**), we first inhibited GABA release with the μ-opioid receptor agonist DAMGO (0.5–1 μM, 77.9 ± 7.3% reduction, $n = 4$; **Supplementary Fig. 6**)[18] and then produced a tonic activation of $GABA_A$ receptors by perfusing the selective agonist muscimol (1 μM; average hyperpolarization, −2.4 ± 0.5 mV; average conductance increase, 4.7 ± 0.3 nS; $n = 4$). In the presence of tonic inhibition, $EPSG_T$ no longer varied with input strength (nonsignificant decrease of 0.003 nS per percentile input strength, $n = 14$, $P = 0.4$; **Fig. 2b**). Thus, the progressive increase in $GABA_A$ receptor activation accounts for the increase in $EPSG_T$. This is supported by the fact that at high input strengths (>0.5), when the amplitude of FFI no longer increased (**Fig. 2a**), $EPSG_T$ remained constant (nonsignificant decrease of 0.02 nS per percentile input strength, $P = 0.4$; **Supplementary Fig. 7**).

By how much does the dynamic $EPSG_T$ increase the range of inputs that the pyramidal cell population responds to? We compared the activation curve of the CA1 pyramidal cell population under control conditions and in the presence of gabazine, where the $EPSG_T$ is fixed (**Fig. 2c**). The number of Schaffer collaterals necessary to recruit the lowest fractions of the pyramidal cell population was comparable in both conditions (for example, 5% recruitment: control, 0.028 input strength; gabazine, 0.03 input strength; **Fig. 2c**). The situation was, however, radically different when larger numbers of Schaffer collaterals were activated. In the presence of gabazine, an approximately eightfold increase in the number of activated Schaffer collaterals readily led to the saturation of the pyramidal cell population (95% recruitment with 0.26 input strength), whereas the same increase in stimulated

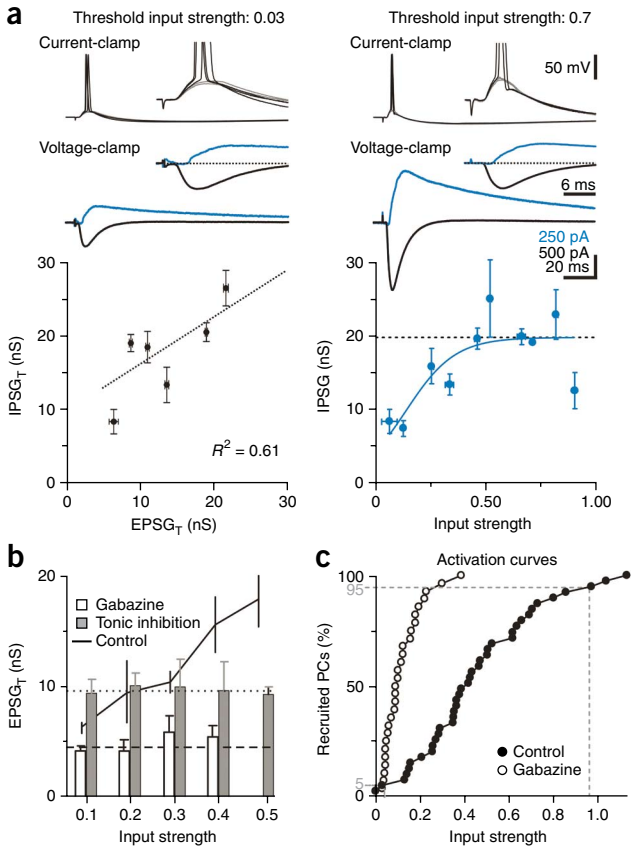

Figure 2 Feedforward inhibition expands the dynamic range of the pyramidal cell population. (**a**) Top traces represent whole-cell current-clamp recording from two CA1 pyramidal cells recruited at threshold by weak (left) or strong (right) Schaffer collateral stimulation (five superimposed sweeps; black indicates successes and gray indicates failures to trigger a spike). Bottom traces, represent threshold EPSC (black, average of five traces recorded in the voltage clamp, −88 and −92 mV for left and right, respectively) and concomitantly evoked feedforward IPSC (blue, recorded at −52 and −59 mV for left and right, respectively, and isolated by subtraction from average of ten sweeps). Insets represent expanded timescale of the sweeps. The size of the two insets has been scaled to match EPSC amplitudes. Bottom left, threshold feedforward IPSG ($IPSG_T$) plotted against $EPSG_T$ (bin width of 2.5 nS, $n = 30$, spike threshold determined in loose patch for $n = 19$ cells and in whole-cell current clamp for $n = 11$ cells, dotted line is the linear regression fit of the binned data, $R^2 = 0.61$, slope of 0.82). Bottom right, feedforward IPSG plotted against input strength (bin width of 0.1, $n = 50$, continuous blue line is a Boltzmann fit of the binned data). Error bars are s.e.m. (**b**) Summary graph of $EPSG_T$s plotted against input strength in the presence of gabazine (6 μM, $n = 30$, spike threshold determined in loose patch for $n = 20$ cells and in whole-cell current clamp for $n = 10$ cells) or under tonic inhibition (1 μM muscimol and 0.5–1 μM DAMGO, $n = 14$, spike threshold determined in loose-patch for $n = 11$ cells and in whole-cell current clamp for $n = 3$ cells). Dotted and dashed horizontal lines represent the average $EPSG_T$ during tonic inhibition or gabazine treatment, respectively. In contrast with control conditions (black line from **Fig. 1b**), the $EPSG_T$ recorded in gabazine or tonic inhibition changed little with increasing input strength. For all input strengths, the $EPSG_T$ during tonic inhibition was larger than during gabazine treatment. (**c**) Activation curves (cumulative distribution of input strengths eliciting 50% spiking) in control conditions (black symbols from **Fig. 1a**) and after gabazine treatment ($n = 28$, spike threshold determined in loose patch for all cells). Dashed lines indicate input strengths recruiting 5% and 95% of the pyramidal cell population. Error bars are s.e.m.

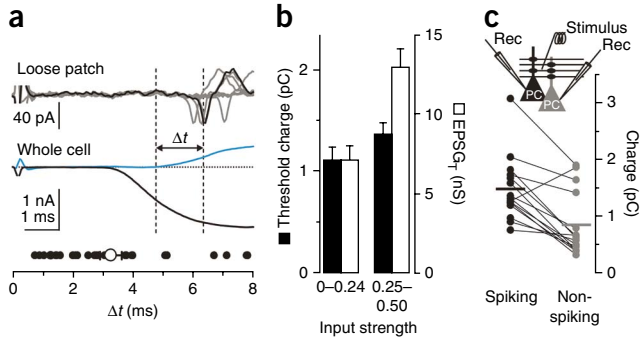

Figure 3 Pyramidal cells spike after the onset of feedforward inhibition. (**a**) Top traces are loose patch recordings from a CA1 pyramidal cell in response to threshold stimulation of Schaffer collaterals (five superimposed sweeps). Bottom traces are voltage-clamp recordings from the same neuron; the EPSC (black line, average of five traces) was recorded at –85 mV and the feedforward IPSC (blue line, isolated by subtraction from average of ten traces) was recorded at –60 mV. The vertical dashed lines mark the onset of the IPSC and the average timing of the spike in the pyramidal cell. The IPSC onset occurred before the spiking of the pyramidal cell. Bottom, summary of 30 similar experiments (spike threshold determined in loose patch for $n = 18$ cells and in whole-cell current clamp for $n = 12$ cells). The open symbol represents the average. (**b**) The net threshold charge (EPSC minus IPSC) entering the cell from the onset of the EPSC to the time of the spike and the $EPSG_T$ are shown for two different ranges of threshold input strengths. The threshold charge did not increase significantly with increasing input strength ($P = 0.3$). In contrast, the peak conductance of the $EPSG_T$ recorded in the same cells was significantly larger for larger input strengths ($P = 0.03$). Error bars represent s.e.m. (**c**) Simultaneous recording from two neighboring pyramidal cells in which Schaffer collaterals stimulation was sufficiently strong to reach threshold in one cell (black), but not in the other (gray, $n = 15$ pairs). The net threshold charge entering in the spiking pyramidal cells was significantly larger than the net charge entering the nonspiking pyramidal cells ($P = 0.004$). Circles represent individual experiments and horizontal lines represent averages.

Schaffer collaterals in control conditions recruited only 19.9% of the population (**Fig. 2c**). Thus, gabazine increased the slope of the activation curve without producing major changes in the offset (**Fig. 2c**). Hence, a dynamic $EPSG_T$ leads to a fourfold expansion of the range of inputs that the CA1 pyramidal cell population can respond to.

FFI arrives before spike

By what mechanism does the feedforward inhibitory postsynaptic current (IPSC) control the size of the $EPSG_T$? We compared the timing of the spike elicited in pyramidal cells by Schaffer collateral stimulation with the onset of the feedforward IPSC. When stimulated at threshold for spike generation, the spike occurred 5.0 ± 0.4 ms after the onset of the EPSC and 3.3 ± 0.4 ms after the onset of the feedforward IPSC ($n = 30$; **Fig. 3a**). The latency between the onset of the EPSC and of the IPSC was 1.65 ± 0.08 ms ($n = 30$), consistent with previous data[15], and did not change with stimulus strength ($R^2 = 0.007$, $P = 0.4$, $n = 30$). Thus, in response to threshold Schaffer collateral stimulation, FFI reached pyramidal cells before the membrane potential of the neuron reached threshold for spike generation.

Over the period preceding the spike, synaptic inhibition overlapped with the EPSC, thereby reducing the excitatory charge entering the cell by 28.1 ± 4.3% ($n = 30$). Specifically, although the integral of the EPSC from its onset to the time of the spike (excitatory charge) averaged 2.2 ± 0.2 pC ($n = 30$), the net synaptic charge (excitatory-inhibitory charge, see Online Methods) entering pyramidal cells was 1.4 ± 0.1 pC ($n = 30$). In contrast to the $EPSG_T$ this net threshold charge was constant and independent of input strength (threshold charge, 1.1 ± 0.1 pC, ($n = 4$) at 0–0.25 input strength versus 1.4 ± 0.1 pC, ($n = 14$) at 0.25–0.5, $P = 0.3$; $EPSG_T$, 7.1 ± 0.9 nS ($n = 4$) at 0–0.25 input strength versus 13.1 ± 1.3 nS ($n = 14$) at 0.25–0.5, $P = 0.03$; **Fig. 3b**). Furthermore, at any given input strength, the threshold charge was significantly larger in pyramidal cells that reached threshold for spike generation as compared with the charge entering over the same time interval in simultaneously recorded cells that did not reach threshold (0.8 ± 0.1 pC, $P = 0.004$, $n = 15$; **Fig. 3c**). In the cells that did not spike, the threshold charge (that is, ~1.5 pC) would have been reached 5.0 ± 0.3 ms after the onset of the EPSC if inhibition had not been present. Thus, by overlapping with excitation before spike occurrence, FFI controls the amplitude of the EPSC necessary to reach spike threshold.

Heterogeneous excitation and homogeneous inhibition

What determines which pyramidal cells in the population are recruited in response to Schaffer collateral stimulation? We recorded from two neighboring pyramidal cells simultaneously (somata separated by ≤50 µm) and increased the number of activated Schaffer collaterals until one of the two cells spiked (**Fig. 4a**). We then compared the EPSGs and feedforward IPSGs in the two cells. Although the EPSG was, on average, 1.6 ± 0.1–fold larger in the cell that spiked ($P = 0.001$, $n = 15$; **Fig. 4b**), the IPSG was, on average, not significantly different between the two neurons (1.1 ± 0.1–fold difference, $P = 0.3$, $n = 15$; **Fig. 4b**). Furthermore, the latency of the feedforward IPSC (with respect to the onset of the EPSC) did not differ significantly between spiking (1.75 ± 0.09 ms) and nonspiking neurons (1.59 ± 0.06 ms, $P = 0.09$, $n = 15$). Thus, differences in the amplitude of synaptic excitation, rather than in the amplitude or timing of inhibition, govern which neuron will spike in response to Schaffer collateral stimulation.

To determine whether inhibition is more homogeneously distributed across pyramidal cells as compared with excitation, we computed the 'spread', that is, the absolute difference in amplitude of simultaneously recorded EPSGs or IPSGs normalized by the average of the amplitudes and divided by two. Although the spread of EPSGs between two simultaneously recorded pyramidal cells was 21 ± 3% ($n = 15$, same paired values as above; **Fig. 4b**), the spread of the concomitant IPSGs was only 11 ± 2% ($P = 0.03$, $n = 15$). We also calculated how well the amplitude of inhibition in one cell correlated with the amplitude of inhibition in its neighbor and did the same for excitation. For this, we used the same paired values as described above (**Fig. 4b**), but we randomly allocated the spiking cell to either one of the two axes (**Fig. 4b**). This randomization removes the correlation bias caused by systematically having the larger amplitude on the same axis. The correlation between IPSGs ($R_{In} = 0.79$) was significantly larger than the correlation between EPSGs ($R_{Ex} = 0.30$, $P < 0.02$, see Online Methods; **Fig. 4b**). Thus, inhibition is more homogeneous than excitation across the pyramidal cell population.

To test whether the relative homogeneity of inhibition with respect to excitation also holds true for individual synaptic events, we compared trial-by-trial fluctuations of the amplitude of EPSC and feedforward IPSC between two simultaneously recorded pyramidal cells (**Fig. 4c**). Using a cesium-based internal solution, we isolated feedforward IPSCs and monosynaptic EPSCs by voltage clamping the cell at the EPSC or IPSC reversal potential, respectively (**Fig. 4c**). The amplitude of the feedforward IPSC covaried between the two recorded neurons (average correlation, $R^2 = 0.26 \pm 0.06$, $n = 5$; **Fig. 4c**). This correlation was significantly less pronounced for monosynaptic EPSCs (average correlation, $R^2 = 0.06 \pm 0.005$, $n = 5$, $P = 0.033$; **Fig. 4c**). These results indicate that, although FFI is